Appl. Magn. Reson. 25, 621–636 (2004)

Applied Magnetic Resonance

Magnetic Resonance Sounding: Enhanced Modeling of a Phase Shift

A. Legchenko

Institut de Recherche pour le Développement, Paris, France

Received July 28, 2003; revised August 14, 2003

Abstract. Magnetic resonance sounding (MRS) is a geophysical method for noninvasive groundwater investigation. A wire loop on the surface is energized by a pulse of oscillating current. After the pulse is cut off, the free induction decay signal from groundwater is measured with the same loop. The Larmor frequency depends on the Earth's magnetic field and varies between 800 and 2800 Hz around the world. Available mathematical models assume that the geomagnetic field is constant and the pulse frequency is equal to the Larmor frequency. These assumptions allow calculation of the phase shift of the signal caused by only the electrical conductivity of the subsurface. However, the existing models are simplified. The Earth's magnetic field may be locally modified by rocks and often is not homogeneous over the volume investigated by MRS. It may also vary in time. A nonconstant geomagnetic field is changing the Larmor frequency at 1 to 5 Hz during one sounding, whilst the pulse frequency is set in the beginning of the sounding. Under these conditions, the assumption of zero frequency offset between the pulse frequency and the Larmor frequency is often unsound. The nonzero frequency offset causes a phase shift in the MRS signal comparable with the shift caused by electrically conductive rocks. For increasing the accuracy of phase shift modeling, an enhanced mathematical model in which the frequency offset is taken into account has been developed. With the enhanced model, the phase of the MRS signal can be calculated with better accuracy. Field measurements reveal a good correlation between experimental and theoretical signals.

1 Introduction

Electrical and electromagnetic methods for noninvasive groundwater investigation are widely used in geophysics for localizing highly permeable water-saturated formations (aquifers). They are based on correlations between the electrical resistivity of a rock and the amount of water in this rock. However, the resistivity depends not only on the water content but also on other factors (origin of rock, mineralogy, water salinity, etc.), which makes interpretation of field measurements nonunique. For example, a resistivity of 50 $\Omega \cdot$ m may equally correspond to chalk, limestone, or water-saturated sand. While water-saturated sand is usually a good aquifer, chalk and limestone may be compact or fractured. When they are compact, the rocks contain very low amount of mobile

water; when they are fractured, they are aquifers. The resistivity of water-saturated rock is also dependent on the water salinity. Consequently, when the water resistivity is around 10 $\Omega \cdot m$, water-saturated sand cannot be distinguished from clay (typically 5–20 $\Omega \cdot m$), which is not an aquifer. The main distinction of the magnetic resonance sounding (MRS) method is that it measures a magnetic resonance signal generated by groundwater molecules. As the signal is directly related to groundwater, the interpretation of field measurements is getting more reliable. For example, MRS allows unambiguously resolving the above discussed sand, chalk, limestone and clay problem.

A mathematical model for computing the amplitude of the MRS signal over insulated earth was initially developed in the former USSR [1]. Later the influence of the electrically conductive subsurface on the phase shift of the MRS signal was taken into account in the model [2]. The accuracy of the phase-shift modeling was recently improved in ref. 3 by considering elliptical polarization of the oscillating electromagnetic field in the subsurface.

All these mathematical models assume that the Earth's magnetic field is constant, the pulse frequency is equal to the Larmor frequency, and only the first harmonic of the pulse is considered. These assumptions allow calculation of the phase shift of the signal caused by only the electrical conductivity of the subsurface. However, the existing models are simplified as follows.

1. The Earth's magnetic field may be locally modified by rocks and often is not homogeneous over a large volume. It may also vary in time, thus changing the Larmor frequency at a few hertz during a day. For an MRS setup with a square loop of 75 by 75 m, a cube of 100 by 100 by 100 m can approximate the volume investigated by MRS. One sounding takes from one to ten hours. Under these conditions, the geomagnetic field cannot be considered as constant, an effect that causes a nonzero frequency offset between the pulse frequency and the Larmor frequency.

2. In order to obtain an adequate signal for the protons in deep water, a sufficiently large flip angle for the nuclear magnetization must be used, requiring the current pulse in the loop to be set as large as possible. However, for larger current the flip angle for protons in shallow water is also large not only for the first but also for the second and third harmonics of the pulse, and they cannot be neglected, as shown below. As the second and the third harmonics are respectively shifted at approximately 35 and 60 Hz from the Larmor frequency, shallow aquifers are irradiated by an oscillating magnetic field with a nonzero frequency offset even if for the first harmonic the frequency is equal to the Larmor frequency.

A growing experience in the MRS application reveals more and more practically important situations when not only the phase shift but even amplitudes cannot be correctly computed with the existing models. Furthermore, the neglect of information about groundwater contained in the phase of the signal is diminishing the MRS performance. In order to improve the accuracy of amplitude and phase shift computation, an enhanced mathematical model has been developed.

This paper is aimed to both nuclear magnetic resonance (NMR) and geophysical communities and in order to facilitate the reading, an elementary review of the NMR principles and the MRS field setup are presented.

2 Background

The MRS field setup consists of a wire loop laid out on the ground, normally in a circle or square with a size of between 10 and 200 m (diameter or side, respectively) [4]. The depth of investigation is proportional to the loop size (Fig. 1). The loop is then energized by a pulse of an alternating current $i(t) = I_0\cos(\omega_0 t)$. The frequency of the current is equal to the Larmor frequency of the protons in the geomagnetic field. The pulse causes precession of spin magnetization of the protons in groundwater around the geomagnetic field, which creates an alternating magnetic field that can be detected with the same loop after the pulse was terminated (the free induction decay method). Oscillating with the Larmor frequency, the MRS signal has an exponential envelope and depends on the pulse moment $q = I_0\tau$ with I_0 and τ being the amplitude and duration of the pulse, respectively. Measurements of the magnetic resonance signal are performed by varying the pulse moment and then the inversion of the data reveals a vertical distribution of the water content in the subsurface. Increase of the water content in the MRS log corresponds to an aquifer.

The macroscopic spin magnetization related to the water distribution in the subsurface varies inside the investigated area, but we can assume the geomagnetic field $\mathbf{B}_0$ and the local macroscopic spin magnetization M to be constant over a small volume dV. In equilibrium, the total spin magnetization of protons is aligned along the geomagnetic field which is in the general case inclined at an angle α and does not produce any measurable electromagnetic signal. With a wire loop on the surface, we now pulse our specimen dV with an oscillating radio-frequency magnetic field $\mathbf{B}_1$ (Fig. 2). Its frequency is chosen to satisfy the spin Larmor resonance condition $\omega = \gamma B_0$, where B_0 is the magnitude of the geomagnetic field and γ is the gyromagnetic ratio for the protons. When using the classical model [5] in the coordinate system rotating with an angular frequency $\omega = -\gamma B_0$, the geomagnetic field is oriented in the z direction $\mathbf{B}_0 = \mathbf{k}B_{0z}$. In the general case, the oscillating magnetic field in the subsurface is elliptically polarized [3]. However, it was shown that working within a one-dimensional (1-D)

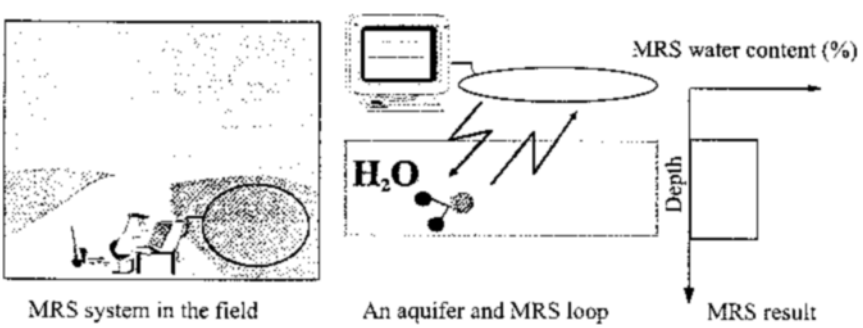

Fig. 1. MRS method for groundwater investigation.

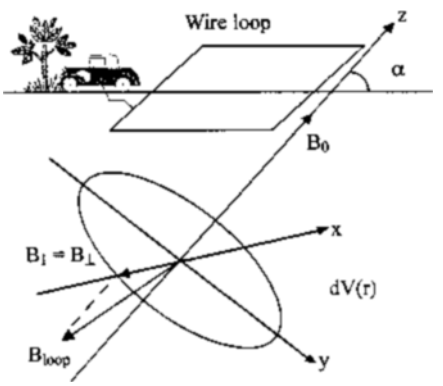

Fig. 2. Oscillating magnetic field (B_1) transmitted by the loop and the geomagnetic field (B_0).

model, elliptical polarization must be taken into account only when the subsurface is very conductive (<2 $\Omega \cdot$ m), the inclination of the geomagnetic field is close to zero, and groundwater is shallow [6]. Thus, when the resistivity of rocks is large than 5–10 $\Omega \cdot$ m, we can still use an approximate formula with linear polarization, the introduced errors being quite small. By assuming the linear polarization, the oscillating magnetic field can be presented as two rotating components in the plane perpendicular to the z-axis, the corotating ($+\omega$) and counterrotating ($-\omega$) components. The effect of the counterrotating component on the spin system is neglected. When $t = 0$, the rotating magnetic field $0.5\mathbf{B}_1$ is oriented in the $-x$ direction (Fig. 2). We assume its magnitude $0.5B_1(x, y, z)$ to be constant in the volume dV. In MRS the rotating frame and the transmitted magnetic field have the same frequency, which is selected after measuring the geomagnetic field on the surface with a proton magnetometer.

Under the exact resonance, the flip angle for the spin magnetization can be expressed as

$$\theta = \frac{1}{2}\gamma B_1 \tau = \frac{1}{2I_0}\gamma B_1 q, \tag{1}$$

where $q = I_0\tau$ is the pulse moment. The transverse component of the spin magnetization $M_\perp$ which creates an alternating magnetic field that can be measured after the pulse cutoff thus becomes

$$M_\perp = M_0 \sin(\theta). \tag{2}$$

M_0 is described by the Curie equation

$$M_0 = NB_0 \frac{\gamma^2 \hbar^2}{4kT}, \tag{3}$$

where N is the number of hydrogen protons per unit volume, T is the absolute temperature, $\hbar$ is the Planck constant and the Boltzmann constant $k = 1.3805 \times 10^{-23}$ J/°. Since $N = 6.692 \cdot 10^{28}$ m^{-3}, it is found that $M_0 = 3.287 \cdot 10^{-3} B_0$ at 293 K (20°C). Neglect of the relaxation during a pulse is not easily justified in rocks. In aquifers, however, the relaxation times are generally sufficiently long, making introduced errors acceptable. If the pulse is applied for a time τ ($\tau \ll T_1$, T_2, T_2^*), where T_1, T_2, T_2^* are the magnetic resonance relaxation times, then the amplitude of the MRS signal can be computed with the existing models [1, 2]. A precessing magnetic moment $M_\perp \mathrm{d}V$ can be represented as a small coil of an area ΔS with a current I_c ($M_\perp \mathrm{d}V = I_c \Delta S$). A magnetic flux through the coil created by a current in the loop I_0 is $\Phi_{c,l} = L_{l,c} I_0$, where $L_{l,c}$ is the coefficient of mutual inductance between the loop and the coil. A magnetic flux through the loop created by the current in the coil I_c is $\mathrm{d}\Phi_{l,c} = L_{c,l} I_c$. With the reciprocity theorem we can write $L_{l,c} = L_{c,l}$ and consequently, $\mathrm{d}\Phi_{l,c} I_0 = \Phi_{c,l} I_c$. By substituting $\Phi_{c,l} = B_1 \Delta S$ and $I_c \Delta S = M_\perp \mathrm{d}V$, we get $\mathrm{d}\Phi_{l,c} I_0 = B_1 I_c \Delta S = B_1 M_\perp \mathrm{d}V$. The differential voltage induced in the loop by the volume $\mathrm{d}V$ and oscillating with the Larmor frequency voltage is

$$\mathrm{d}e = -\frac{\partial}{\partial t}\mathrm{d}\Phi_{l,c} = -\frac{\partial}{\partial t}\left(\frac{B_1}{I_0} M_\perp \exp(-j\omega_0 t)\mathrm{d}V\right) = j\exp(-j\omega_0 t)\frac{\omega_0 B_1}{I_0} M_\perp \mathrm{d}V.$$

The signal induced in the receiver loop $e = e_0(q) j \exp(-j\omega_0 t)$ is proportional to the sum of the flux of all precessing magnetic moments and thus

$$e_0(q) = \frac{\omega_0}{I_0}\int_V B_1(\mathbf{r}) \exp(j2\varphi_\rho(\mathbf{r})) M_\perp(q, \mathbf{r}) w(\mathbf{r}) \mathrm{d}V(\mathbf{r}), \tag{4}$$

where $B_1(\mathbf{r})$ is the transmitted magnetic field component perpendicular to the geomagnetic field, $0 \leqslant w(\mathbf{r}) \leqslant 1$ is the water content, and $\mathbf{r} = r(x, y, z)$ is the coordinate vector. The phase shift φ_ρ of the transmitting magnetic field relative to the current in the loop is caused by the electrical conductivity of the subsurface. The double shift is due to the shift of the transmitting and receiving fields which are equal when the coincident loop is applied.

The magnetic field transmitted by the loop can be represented as $B_1 = \beta_1 I_0$, with β_1 being the field per unit current. From Eq. (4) one can see that the signal is proportional to $\beta_1 = B_1/I_0$ rather than to B_1. That means that the maximum value of the signal can be achieved when $\theta = \pi/2$, and depends on the mutual inductance between the loop and groundwater which in turn depends on the loop size and groundwater depth. The increase of the transmitted power will not increase the signal over its maximum value proportional to M_0 and the geometry of the loop-aquifer system. Equation (4) is a mathematical expression of the existing models of MRS.

3 MRS Phase Shift

In practice, the assumption of $\Delta\omega = 0$ is not always justified. As the geomagnetic field might be not constant over the investigated volume, the Larmor frequency ω_0 will also vary. Thus,

$$\Delta\omega = \omega_0 - \omega = \gamma(B_0 + \Delta B_0(x, y, z)) - \omega \neq 0 .$$

If $\Delta\omega \neq 0$, then according to the Bloch equations, in the volume dV the motion of spins in the rotating frame follows a precession cone around the effective field $\mathbf{B}_{\text{eff}} = 0.5\mathbf{B}_1 + \mathbf{k}(B_0 - \omega/\gamma)$.

The total precession angle θ of the spins given by Eq. (2) should be replaced by $\theta = \gamma B_{\text{eff}}\tau = \omega_{\text{eff}}\tau$, where $\omega_{\text{eff}}^2 = \omega_1^2 + \Delta\omega^2$, in which $\omega_1 = 0.5\gamma B_1$.

The transverse component of the spin magnetization $M_\perp^2 = M_x^2 + M_y^2$ creates an alternating magnetic field that can be measured after the pulse cutoff. At time $t = \tau$, in general, it will have three components [7]

$$M_x = -\frac{\omega_1 \Delta\omega}{\omega_{\text{eff}}^2}(1 - \cos(\omega_{\text{eff}}\tau))M_0 , \tag{5}$$

$$M_y = \frac{\omega_1}{\omega_{\text{eff}}}\sin(\omega_{\text{eff}}\tau)M_0 , \tag{6}$$

$$M_z = \frac{\Delta\omega^2 + \omega_1^2\cos(\omega_{\text{eff}}\tau)}{\omega_{\text{eff}}^2}M_0 .$$

The behavior of the elemental spin magnetization for different frequency offsets is shown in Fig. 3. When $\Delta\omega = 0$, the M_x component corresponding to the imaginary part of the MRS signal is zero and hence the signal, which is thus proportional only to M_y, is real. Otherwise it is complex.

A phase shift of the magnetic field B_1 caused by the electrical conductivity of rocks also creates a phase shift of the MRS response. Considering that both the magnetic field generated by spin magnetization and the transmitted magnetic field B_1 are complex, and assuming a coincident transmitting-receiving loop, we can express the phase of the signal generated by the volume dV as

$$\varphi_0 = \tan^{-1}(M_x / M_y) + 2\tan^{-1}(B_{1x} / B_{1y}) = \varphi_{\Delta\omega} + 2\varphi_\rho , \tag{7}$$

where $\varphi_{\Delta\omega}$ and φ_ρ are the phase shifts due to the frequency offset and the electromagnetic shift caused by the electrical conductivity of rocks, respectively.

Now, let us look at the current pulse that energizes the loop

$$i(t) = G(t)I_0\cos(\omega_0 t), \quad 0 < t \leq \tau ,$$

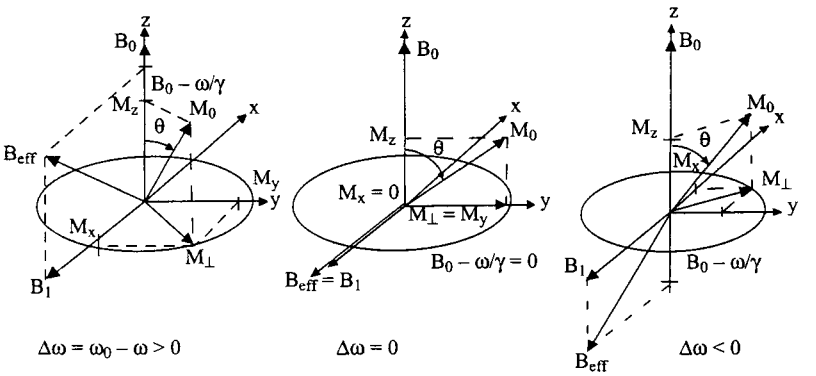

Fig. 3. Precession of spin magnetization in the tilted rotating reference frame.

where $G(t)$ is a shape of the envelope of the pulse, and I_0 and τ are its amplitude and duration, respectively. The frequency of the current is selected to be as close as possible to the Larmor frequency of the protons in the geomagnetic field $f_0 = \omega_0/2\pi = \gamma B_0/2\pi$ Hz, the frequency of which depends on the geographical location of the investigated area and varies between 800 and 2800 Hz around the globe.

The Fourier spectrum of the rectangular pulse is well known,

$$F(\omega) = \tau \frac{\sin(\omega\tau/2)}{\omega\tau/2}.$$

While for a rectangular pulse $G(t) = 1$, the real pulses generated by MRS equipment generally are not rectangular. $G(t)$ is not constant and depends on the frequency, generator setup, loop size, and on the electrical conductivity of the subsurface. Both real and imaginary parts of the Fourier spectra depend on the pulse envelope (Fig. 4).

These spectra show that the amplitude of the second harmonic is about 20% of that of the first one and the frequency offset is about 35 Hz. As the magnitude of the current is limited, in deep water irradiated from the surface the flip angle of spin magnetization is small even for the first harmonic. That means that water in deep aquifers mostly responds to the first harmonic and effects of higher harmonics on the MRS signal can be neglected. In water close to the surface, however, the flip angle caused by higher harmonics is significant and they must be taken into account. Consequently, in the case of exact resonance ($\Delta\omega = 0$) and nonconductive rocks the MRS signal generated by deep water may be real; for shallow aquifers, however, more than one harmonic of the pulse that have nonzero frequency offset must be considered and hence the signal is always complex. It has been experimentally shown that even for a large frequency offset ($\Delta\omega/2\pi = 100$ Hz), the magnetic resonance signal from groundwater can be measured by MRS instrument [8]. Thus, at least three first harmonics of the pulse should be taken into account.

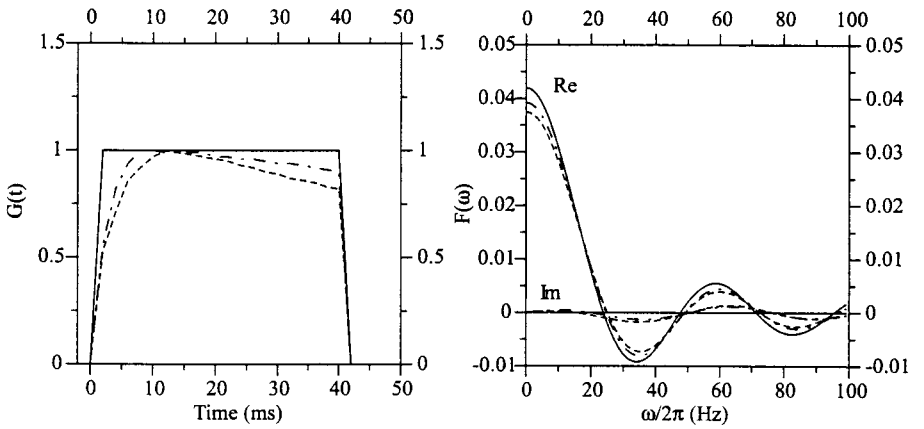

Fig. 4. Rectangular pulse and real pulses transmitted by MRS equipment. Solid line, rectangular pulse; dashed line, real pulse 1; dashed-dotted line, real pulse 2.

We assume the spin system to be linear, which is an approximation, but it allows calculating the MRS response with the first three harmonics generated by the pulse. As the frequency offset between first three harmonics is relatively small (about 80 Hz), we can approximate with sufficient accuracy $B_1(\mathbf{r})/I_0 = B_{1k}(\mathbf{r})/I_{0k}$, where $B_{1k}(\mathbf{r})$ is the transmitted by kth harmonic magnetic field and I_{0k} is the amplitude of this harmonic. By employing a similar approach as was used for developing Eq. (4) and considering the pulse harmonics, the induced voltage in the receiving loop becomes

$$e_0(q) = \frac{\omega_0}{I_0}\int_V B_1(\mathbf{r})\sum_{k=1}^{K}\left(\exp(j\varphi_{0k}(\mathbf{r}))M_{\perp k}(q,\mathbf{r})\right)w(\mathbf{r})\mathrm{d}V(\mathbf{r}), \tag{8}$$

where φ_{0k} is given by Eq. (7) and $M_{\perp k}(q,\mathbf{r}) = (M_{xk}^2 + M_{yk}^2)^{1/2}$ by Eqs. (5) and (6) for each harmonic with the corresponding frequency offset $\Delta\omega_k$, and K being the number of harmonics.

Water distribution in the subsurface $w(\mathbf{r})$ is the solution of Eqs. (4) or (8). By assuming the horizontal stratification and electrical conductivity of the subsurface to be known, the problem can be simplified to one dimension, and its solution then provides the vertical distribution of water content $w(z)$. An inversion algorithm for inverting amplitudes can be found in ref. 9. By replacing Eq. (4) by Eq. (8), the phase shift can be calculated with better accuracy and consequently the complex signals can be also inverted.

Practically, the vertical distribution of electrical conductivity in the subsurface $\rho(z)$ can be measured with one of the electrical or electrical-magnetic methods widely used in geophysics; and the apparent frequency offset $\Delta\omega(q)$ can be estimated from MRS data $\Delta\omega(q) = \omega_s(q) - \omega$, where $\omega_s(q)$ is the angular frequency of the received MRS signal and ω that of the rotating frame. Knowledge of $\omega(q)$ and $\rho(z)$ allows calculating the MRS signal.

4 Modeling Results

The MRS signal was calculated with Eq. (8). This mathematical model will be later referred to as the enhanced model. Results were compared with the signal calculated by the existing mathematical model (Eq. (4)), which considers neither the frequency offset nor the full spectrum of the transmitting pulse. Calculations were carried out for a square loop with the side of 75 m, an inclination of the geomagnetic field of 60 degrees, and a Larmor frequency of 2000 Hz. As the practically available pulse moment is limited by 12000 A · ms, all the calculations were also limited by this value. A 5 m thick water layer (w = 20%) with the depth to the top of layer set at 5 and 70 m in a half-space of 100 and 10 Ω · m is assumed.

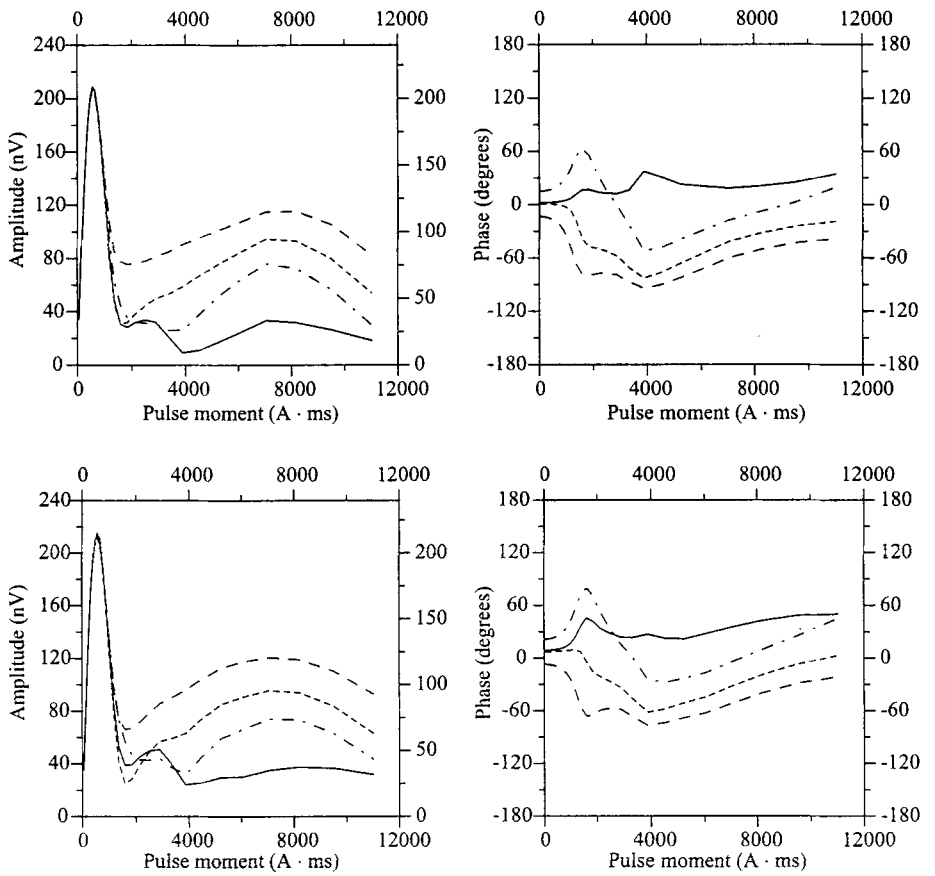

Fig. 5. Complex MRS signal from a 5 m thick water-saturated layer at a depth of 5 m with 20% of the water content computed in 100 Ω · m half-space (top) and 10 Ω · m half-space (bottom). The signal calculated by the existing model is shown by the solid line. Enhanced model: short-dashed line, $\Delta f = 0$; long-dashed line, $\Delta f = 2$ Hz; dashed-dotted line, $\Delta f = -2$ Hz.

Modeling results show that for a shallow layer, the initial part of the amplitude versus the pulse moment is practically equal for both models in nonconductive and conductive half-space (Fig. 5). For larger pulse moments, we observe a strong dependence of the amplitude on the frequency offset. The phase also depends on the frequency offset and the phase shift is significant even in insulating earth. However, one can see that when water is deep, the influence of the frequency offset on the phase shift is small (Fig. 6). Consequently, the phase shift for deep water depends mainly on the electrical conductivity of the rocks.

In the presence of shallow and deep aquifers, the phase depends on both the frequency offset and the electrical conductivity of the rocks. Neglecting this complicated phase behavior might lead to serious errors in interpretation. For example, by comparing the examples presented in Figs. 5 and 6, one can see that

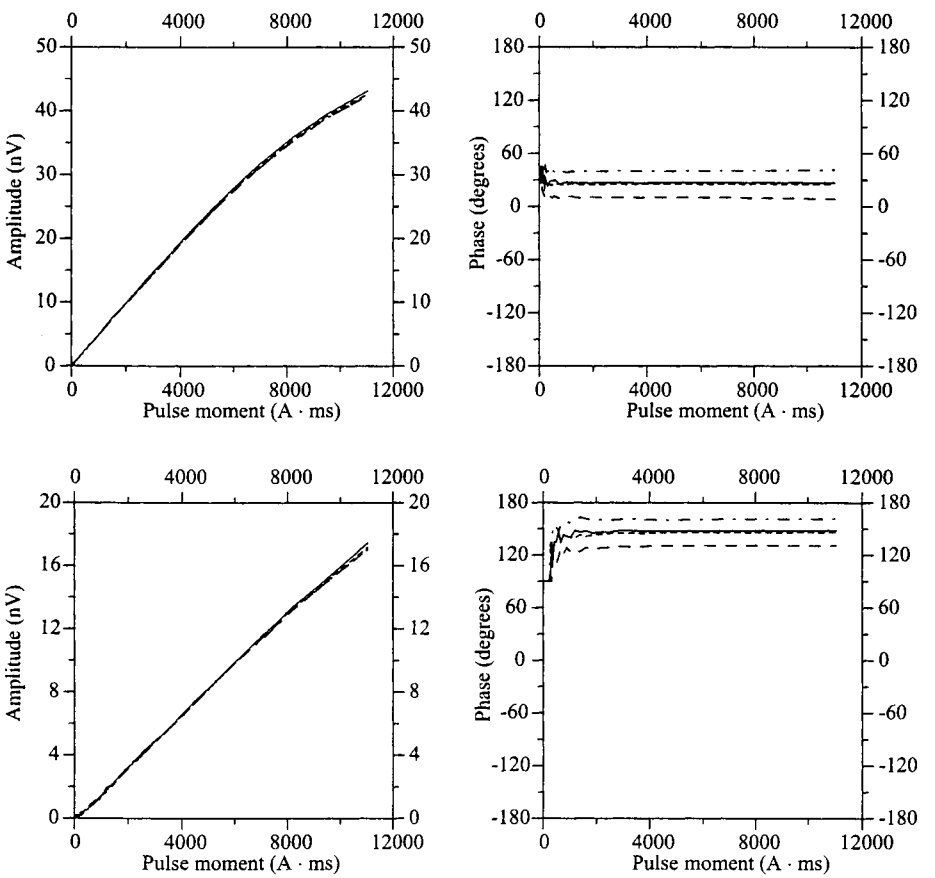

Fig. 6. Complex MRS signal from a 5 m thick water-saturated layer at a depth of 70 m with 20% of the water content computed in 100 Ω · m half-space (top) and 10 Ω · m half-space (bottom). The signal calculated by the existing model is shown by the solid line. Enhanced model: short-dashed line, $\Delta f = 0$; long-dashed line, $\Delta f = 2$ Hz; dashed-dotted line. $\Delta f = -2$ Hz.

for larger pulses the phase of the signal from a shallow layer is negative and the phase shift for a deep layer caused by the electrically conductive rocks is positive. Obviously, under some conditions the signal from this deep layer can be offset by the signal from the shallow layer.

5 Experimental Results

In the framework of scientific cooperation between the Bureau de Recherches Géologiques et Minières (BRGM, Orléans, France) and the U.S. Geological Survey (USGS), MRS measurements were carried out in Haddam Meadows (Connecticut) area in November 2000. This site was used earlier through a collaboration of the USGS; U.S. Environmental Protection Agency; the Institute of Chemical Kinetics and Combustion, Russian Academy of Sciences (ICKC, Novosibirsk, Russia); and the firm Hydrogeotom (Moscow, Russia) as a test site for the MRS technique in 1993 [10]. Ten boreholes are available in this area. The interpretation of the core data, with the aid of ground-penetrating radar, was that the progressive retreat of the glaciers, in a northwesterly direction, left the following structure: (i) bedrock overlain by till that changes upwards into poorly sorted ice marginal deposits, which are in turn overlain by deltaic deposits; (ii) an erosional surface cutting into the previous deltaic deposits; (iii) recent (Holocene) river deposits overlying the remaining glacial sediments.

This complex glacial and post-glacial history can explain the significant lateral variations and mixture of different geological formations revealed by the bore holes in this area. For example, the qualitative information left out of the generalized log of TH-23 well indicates that the gravel interval is "dirty" or poorly sorted. A general trend of coarsening of glacial deposits with depth is observed in the well and test hole data. Available logs provide no information on the increasing volume fraction of water with depth and are too shallow to verify the configuration of the bedrock surface. One well reached bedrock at approximately 43 m. Well data indicate the water table at about 2 m below the surface, slightly less than the elevation of the surface (2.8 ± 0.5 m) above the sea level (river level) at the site.

Nine soundings were performed by BRGM and USGS in 2000 with a NUMIS^{plus} MRS tool developed by IRIS Instruments (France) in cooperation with BRGM and ICKC. Because of a power line passing by, the noise-reducing figure-eight loop was used. The loop is composed of two squares each with 37.5 m long sides [11]. With this loop, the depth of investigation was about 40 m, and the investigated area can be approximated by a parallelepiped of about 60 by 120 by 40 m.

Large variations in the amplitude of the magnetic resonance signal around the Haddam Meadows area were observed. Two MRS measurements near boreholes are presented in Fig. 7. The distance between these stations is about 800 m. Borehole TH-23 reveals a coarse material (gravel) between 8 and 20 m which may be a potential aquifer. However, borehole data indicate that this gravel layer is filled by a very fine glacial material (till) which makes the MRS signal very short,

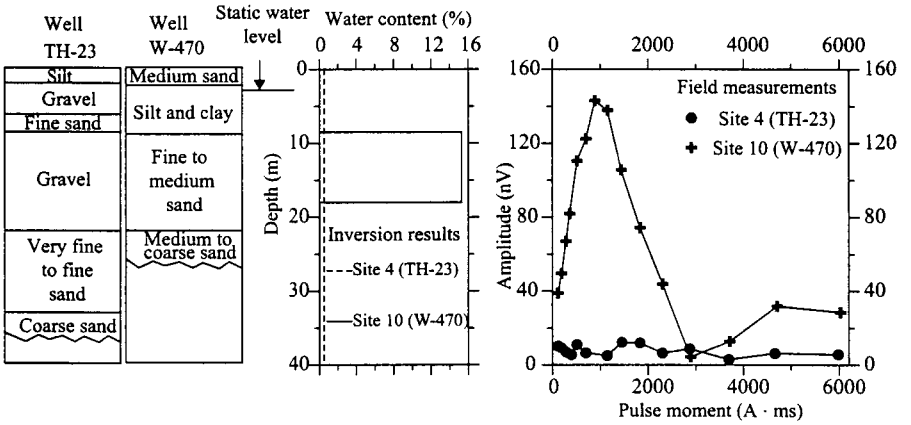

Fig. 7. Haddam Meadows experiments: example of borehole logs and MRS results.

and thus water cannot be detected by MRS in this formation (site 4). A fine-to-medium sand aquifer revealed by borehole W-470 was reliably detected by MRS (site 10). By comparing these results, we presume that in the Haddam Meadows area coarse material is filled by till and thus is not an aquifer as well as silt and clay formations. The medium-to-fine sand however is an aquifer. The depth of groundwater derived from MRS is inconsistent with the water level revealed by boreholes because there is a small percentage of free water in very fine-to-medium materials (silt and clay), and MRS is not able to detect bound water.

When using the existing mathematical model and two water-saturated layers, we observe a good correspondence between experimental and theoretical amplitudes (Fig. 8). But we still have a major problem for fitting the phase. When

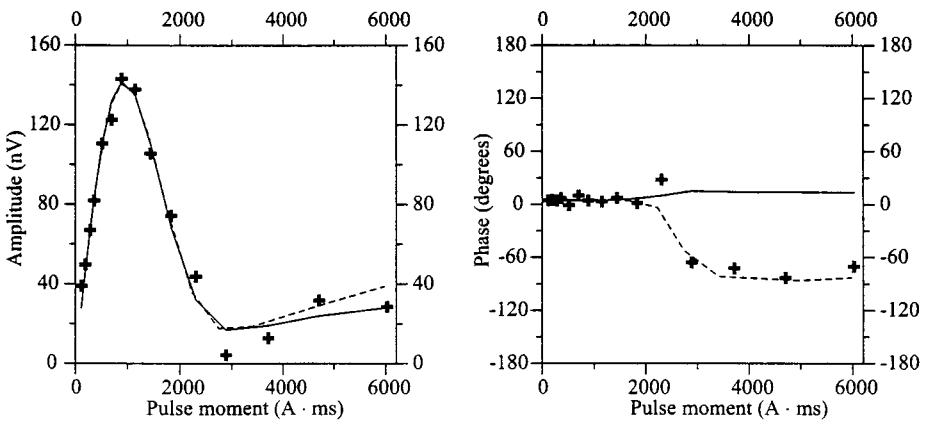

Fig. 8. Haddam Meadows experiments: fitting of experimental signal with the existing and enhanced models. Crosses, field experiment. Solid line, existing model; layer 1: 8.5–17 m, w = 16%; layer 2: 35–42 m, w = 6.5%. Dashed line, enhanced model; layer 1: 8.5–18 m, w = 15.3%.

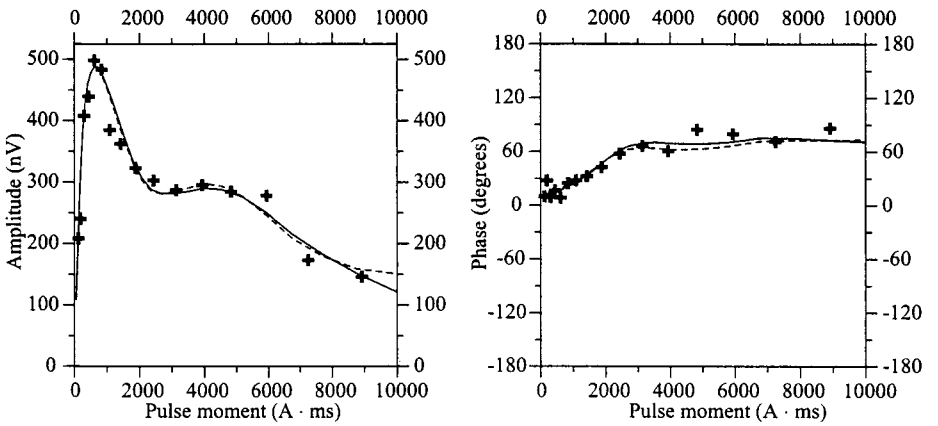

Fig. 9. Saint-Cyr-en-Val experiments: fitting of experimental signal with the existing and enhanced models. Crosses, field experiment. Solid line, existing model; layer 1: 1.8–17.5 m, $w = 16\%$; layer 2: 33–50 m, $w = 13.6\%$. Dashed line, enhanced model; layer 1: 1.8–17 m, $w = 14.6\%$; layer 2: 31–44 m, $w = 17.4\%$; layer 3: 57–98 m, $w = 16.2\%$.

using the enhanced model and just a single water-saturated layer, both the amplitude and phase measured in the field show good matches with the theoretical signal when the transmitting frequency is correctly set at $\Delta\omega = 0$. Available ground truth does not allow to directly confirm that there are no aquifers below 20 m: a special borehole would be required. However, taking into account all available geological information about the site, it can be concluded that the second layer revealed by the interpretation with the existing model does not exist in reality.

A similar problem in the interpretation of experimental data by the existing model was reported in ref. 12. This problem was also resolved when the enhanced model was applied [13].

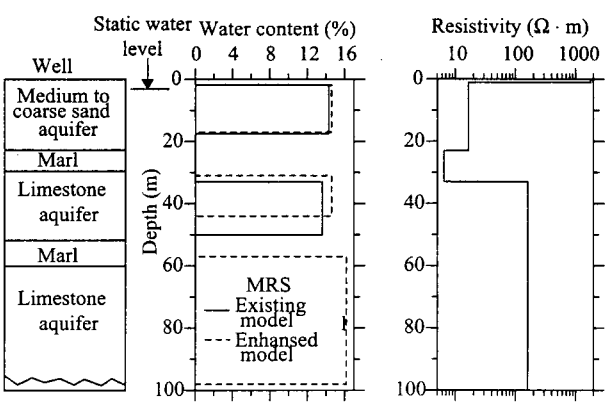

Fig. 10. Saint-Cyr-en-Val experiments: borehole log, TDEM and MRS results.

For MRS measurements carried out in the Saint-Cyr-en-Val area (France), a square loop with 100 m long sides was used. The reliable depth of investigation for this loop is about 100–120 meters. Information about the resistivity distribution was obtained by the time-domain electromagnetic method. Results of the interpretation are presented in Fig. 9. The field data can be equally well fit by the existing model and two aquifers and by the enhanced model and three aquifers. A comparison with the borehole at this site which reveals three aquifers separated by marl layers (Fig. 10) confirms that the result given by the enhanced model is more accurate.

6 Discussion

In the early stage of MRS development (early 1990s), use of a simplified mathematical model was easily justified. Difficulties with the hardware development did not allow measuring accurately the phase of the MRS response, and also the pulse generator was not powerful enough, limiting the power of transmitting pulses. Some measurements for which a disagreement was observed between experimental data and modeling results were put aside because of uncertainty about the accuracy of measurements as well as about the influence of rock electrical conductivity on MRS signal. Today, a new generation of MRS instruments is proven to be more accurate and powerful, and a theory has been developed to take the electrically conductive subsurface into account. However, increasing application of MRS in different geological formations revealed a growing number of field measurements that cannot be correctly modeled by the existing (simplified) model, even when taking into account phase shifts caused by electrically conductive rocks. In many cases these difficulties were resolved when the enhanced model was applied.

With the enhanced model it was shown that in addition to the electrical conductivity of the subsurface two factors may influence MRS measurements: the higher harmonics of the pulse and space-time variations in the geomagnetic field. The weight of each of these factors depends on the geometry of the subsurface and measuring conditions.

If a water-saturated layer is deep and/or the power of the pulse is relatively small, then the pulse harmonics can be neglected. This explains why many soundings can be correctly interpreted by the available simplified models.

If only a shallow aquifer is present, then the pulse harmonics and varying geomagnetic field must be taken into account. Otherwise, the theoretical data will be inconsistent with the measurements and the interpretation by the existing models may incorrectly reveal a deep aquifer.

The most complicated case is when measurements are carried out over two or more aquifers in an electrically conductive subsurface. In this case, all the three factors contribute to the phase shift. A relatively small phase shift caused by variations in the geomagnetic field can be positive or negative, depending on the sign of the offset between the transmitted field frequency and the Larmor

frequency. The pulse harmonics cause a negative phase shift and the electrical conductivity of the rocks a positive phase shift. The measured signal is the sum of complex signals from all the aquifers and under some conditions the effect of mutual elimination of the signal from some of the aquifers is taking place. Neglect of these effects may lead to an erroneous estimation of the water distribution in the subsurface and consequently to an erroneous interpretation of the experimental data. Considering the field example presented in Figs. 9 and 10, one can see that such cancellation might be almost perfect and users of the existing simplified models will not even suspect that there is a problem with the interpretation.

When the enhanced mathematical model is used, both the amplitude and phase of magnetic resonance signals can be calculated more accurately. Inversion of field measurements should be carried out also considering the complex signal and, thus, additional information about groundwater contained in the signal can be extracted.

Two field examples are presented for demonstration purposes only, but the modeling results were verified with a much greater number of field measurements to provide experimental confirmation of the newly developed model.

7 Conclusions

An enhanced model for more accurate computing of the phase shift in the MRS signal has been developed. This model is adapted to the presence of shallow water and geomagnetic field that may be not constant during the measuring time throughout the investigated volume. Field measurements reveal a good correlation between results obtained by the enhanced model and available geophysical and borehole data.

Modeling results demonstrate that not only electrically conductive rocks but also variations in the geomagnetic field and higher harmonics of the pulse can cause phase shifts in the MRS signal. Both modeling and experimental results show that when the existing model is used, then under some conditions the neglect of these effects might lead to such errors in interpretation as false positive or missing aquifers. The enhanced model in these cases allows one to avoid the problems.

Acknowledgements

I thank Eric White of USGS for taking part in the Haddam Meadows experiments and Yves Albouy of IRD (France) for performing measurements by the time-domain electromagnetic method in the Saint-Cyr-en-Val area. Presented results were obtained in the framework of the BRGM research program.

References

1. Pusep A.Yu., Bashurova V.S., Shokhirev N.V., Burshtein A.I. in: Software Development for the NMR Tomography of Sub-Surface Water-Bearing Horizons, p. 89. Novosibirsk: USSR Academy of Sciences 1991.
2. Shushakov O.A.: Geophysics **61**, 998–1006 (1996)
3. Weichman P.B., Lavely E.M., Ritzwoller M.H.: Phys. Rev. E **62**, 1290–1312 (2000)
4. Legchenko A., Valla P.: J. Appl. Geophys. **50**, 3–19 (2002)
5. Abragam A.: The Principles of Nuclear Magnetism, p. 600. Oxford: Oxford University Press 1961.
6. Valla P., Legchenko A.: J. Appl. Geophys. **50**, 217–229 (2002)
7. Mansfield P., Maudsley A.A., Morris P.G., Pykett I.L.: J. Magn. Reson. **33**, 261–274 (1979)
8. Trushkin D.V., Shushakov O.A., Legchenko A.V.: Appl. Magn. Reson. **5**, 399–406 (1993)
9. Legchenko A.V., Shushakov O.A.: Geophysics **63**, 75–84 (1998)
10. Lieblich D.A., Legchenko A., Haeni F.P., Portselan A. in: Proceedings of the Symposium on the Application of Geophysics to Engineering and Environmental Problems, March 27–31, 1994, Boston, Massachusetts, USA, vol. 2, pp. 717–736.
11. Trushkin D.V., Shushakov O.A., Legchenko A.V.: Geophys. Prospect. **42**, 855–862 (1994)
12. Weichman P.B., Dong Rong Lun, Ritzwoller M.H., Lavely E.M.: J. Appl. Geophys. **50**, 129–147 (2002)
13. Legchenko A., Baltassat J.-M., Vouillamoz J.-M. in: Proceedings of the Symposium on the Application of Geophysics to Engineering and Environmental Problems, April 6–10, 2003, San Antonio, Texas, USA, pp. 739–757.

Author's address: Anatoly Legchenko, Institut de Recherche pour le Développement, 32, avenue Henri Varagnat, 93143 Bondy Cedex, France
E-mail: anatoly.legtchenko@bondy.ird.fr